PBFA II, THE PULSED POWER CHARACTERIZATION PHASE

T. H. Martin, B. N. Turman, S. A. Goldstein, J. M. Wilson, D. L. Cook
D. H. McDaniel, E. L. Burgess, G. E. Rochau, E. L. Neau and D. R. Humphreys
Sandia National Laboratories
Albuquerque, NM 87185

Abstract

The Particle Beam Fusion Accelerator II, PBFA II, is now the largest pulsed power device in operation. This paper will summarize its first year and a half of operation for the Department of Energy (DOE) Inertial Confinement Fusion (ICF) program. Thirty-six separate modules provide 72 output pulses that combine to form a 100 TW output pulse at the accelerator center. PBFA II was successfully test fired for the first time on December 11, 1985. This test completed the construction phase (Phase 1) within the expected schedule and budget. The accelerator checkout phase then started (Phase 2). The first priority during checkout was to bring the Phase 1 subsystems into full operation. The accelerator was first tested to determine overall system performance. Next, we modified subsystems that were not performing adequately. The accelerator is now being used for ion diode studies.

Introduction

The Particle Beam Fusion Accelerator II (PBFA II) is now the largest pulsed power device of its kind in operation. It has completed the first pulsed power check out phase (Phase 2) and is now being used primarily for ion diode experiments. Phase 1, the construction phase, started in late 1979 and was completed at the first test firing of the accelerator on December 11, 1985. The nominally 100 TW accelerator was finished six weeks ahead of schedule and within the estimated cost of 48.15 M$, which included new building construction. Phase 2 started after the first test firing and concluded October 1, 1986. Since October 1986, the accelerator has been used primarily for ion diode experiments. The accelerator has also been generating pulsed power data, and further accelerator improvements have been made. After the first shot, we found that most of the accelerator systems operated well. One major subsystem, the 13 MJ energy storage system, was evaluated prior to the first shot. However, we knew that several systems were not easily scalable from PBFA II modeling. Checkout of these systems was then performed by assigning the testing capability of the entire accelerator to checking that specific system. Systems needing to be tested in this manner were the Laser Triggered Switches (LTS), voltage adder, and the Plasma Opening Switches (POS). This paper describes tests and items of interest on PBFA II and provides information that should be useful for other large accelerators. The data are provided in this paper in a sequence starting at the outside of the accelerator and going toward the center. Several other PBFA II papers presented at this conference provide further detail of the PBFA II subsystems. References are made to these papers when appropriate.

There are several significant pulsed power advances in PBFA II:

1. Water is used for the pulse forming and power transmission lines to generate pulsed voltages above 10 MV resulting in a compact accelerator.

2. Thirty-six Marx generators constituting 13 MJ of stored energy were repeatably fired with less than 40 ns total spread. The prefire rate of this large Marx system is very low, below .05 per charge cycle.

3. The gas switch laser trigger system, with the proper optics design, was shown to be a viable and survivable triggering system. Even though large water switching shocks are present, the optics required only minor adjustment between shots.

4. Thirty-six 5 MV laser triggered multichannel gas switches were operated together. Although further modifications are needed, this large, crucial system is feasible. LTS systems have proven their value for large multimodule, pulsed power devices.

5. High voltage (about 5 MV) water switches can be successfully operated without large energy losses and with low jitter if high fields are used.

6. A system using the vacuum insulator stack and the voltage adders as an inductive energy store has been charged to voltages of 12 MV and stored energies greater than 2 MJ at short circuit currents exceeding 6 MA.

7. The POS, in conjunction with a plasma filled blade load, has provided current rise rates of about 2×10^{14} amps per second on one half of the accelerator.

8. Early data was gathered on the performance of ion diodes.

PBFA II Design

A drawing of PBFA II is shown in Fig. 1. The accelerator insulating sections are divided into three main types: oil, water, and vacuum. First the energy storage section, which consists of the Marx generators and their trigger systems, are insulated using a 33 meter (108 ft.) outside diameter ring filled with 2×10^6 lit. (530,000 gal.) of transformer oil. Next the pulse forming section, consisting of laser triggered gas switches, pulse forming lines 1 and 2, water switches, coaxial to flat plate transition, polarity invertors, and the voltage step-up transformers are located in the 2.2×10^6 lit. (580,000 gal.) water section. Finally, the vacuum section is located inside of the (3.7 m diameter, 4.8 m high) insulator stack and contains the inductive store, voltage adders, plasma opening switches, and ion diode.

Marx Generator

The PBFA II prime energy store consists of 36 individual Marx generators that are operated in parallel [1,2,3]. The PBFA II Marx is shown in Fig. 2. The Marx generator design is the latest and most highly synchronized of a series of Sandia designs that started with Hydra, a pulsed power simulator [4]. Each Marx has 60, 1.3 μfd 100 kV energy storage capacitors that are charged in parallel and discharged in series by 30 triggered SF-6 insulated spark gaps that operate reliably without prefires at the nominal charge voltage. Each Marx is operated at a nominal 95 kV charge which provides 360 kJ from each Marx and a total of 13 MJ for the system. The 36 Marx generators are triggered by a fan out trigger system. One main trigger amplifier triggers 9 Marx-type trigger generators. Each trigger generator in turn delivers a 540 kV, 80 nsec risetime pulse to 4 Marx generators.

When the Marx energy storage capacitors are connected in series, the energy is transferred from the oil section into the water capacitors. While transferring the stored energy, the current through the series Marx gaps rises in a sinusoidal manner to a peak current of 110 kA in 0.6 microseconds and then

Report Documentation Page

Form Approved
OMB No. 0704-0188

1. REPORT DATE	2. REPORT TYPE	3. DATES COVERED
JUN 1987	**N/A**	**-**

4. TITLE AND SUBTITLE	5a. CONTRACT NUMBER
PBFA II, The Pulsed Power Characterization Phase 30	5b. GRANT NUMBER
	5c. PROGRAM ELEMENT NUMBER
6. AUTHOR(S)	5d. PROJECT NUMBER
	5e. TASK NUMBER
	5f. WORK UNIT NUMBER
7. PERFORMING ORGANIZATION NAME(S) AND ADDRESS(ES) **Sandia National Laboratories Albuquerque, NM 87185**	8. PERFORMING ORGANIZATION REPORT NUMBER
9. SPONSORING/MONITORING AGENCY NAME(S) AND ADDRESS(ES)	10. SPONSOR/MONITOR'S ACRONYM(S)
	11. SPONSOR/MONITOR'S REPORT NUMBER(S)

12. DISTRIBUTION/AVAILABILITY STATEMENT
Approved for public release, distribution unlimited

13. SUPPLEMENTARY NOTES
See also ADM002371. 2013 IEEE Pulsed Power Conference, Digest of Technical Papers 1976-2013, and Abstracts of the 2013 IEEE International Conference on Plasma Science. Held in San Francisco, CA on 16-21 June 2013. U.S. Government or Federal Purpose Rights License

14. ABSTRACT
The Particle Beam Fusion Accelerator II, PBFA II, is now the largest pulsed power device in operation. This paper will summarize its first year and a half of operation for the Department of Energy (DOE) Inertial Confinement Fusion (ICF) program. Thirty-six separate modules provide 72 output pulses that combine to form a 100 TY output pulse at the accelerator center. PBFA II was successfully test fired for the first time on December 11, 1985. This test completed the construction phase (Phase 1) within the expected schedule and budget. The accelerator checkout phase then started (Phase 2). The first priority during checkout was to bring the Phase 1 subsystems into full operation. The accelerator was first tested to determine overall system performance. Next, we modified subsystems that were not performing adequately. The accelerator is now being used for ion diode studies.

15. SUBJECT TERMS

16. SECURITY CLASSIFICATION OF:			17. LIMITATION OF ABSTRACT	18. NUMBER OF PAGES	19a. NAME OF RESPONSIBLE PERSON
a. REPORT	b. ABSTRACT	c. THIS PAGE			
unclassified	**unclassified**	**unclassified**	**SAR**	**8**	

Standard Form 298 (Rev. 8-98)
Prescribed by ANSI Std Z39-18

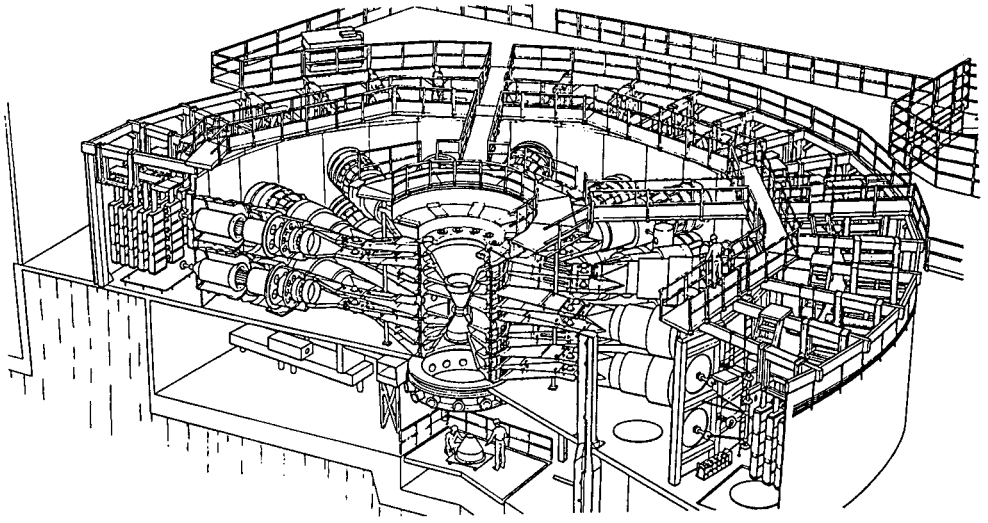

Figure 1 - PBFA II Line Drawing.

decreases toward zero in an additional 0.6 microseconds. Just before the zero current and near peak energy transfer, the laser-triggered gas switches fire and discharge the water capacitors.

The power during Marx-to-water capacitor transfer time is about 13 TW. Since the Marx is charged in about 100 seconds and discharged in one microsecond, the pulse compression ratio of this section is 10^8, which makes the Marx the most efficient and compact pulse compression device in the accelerator.

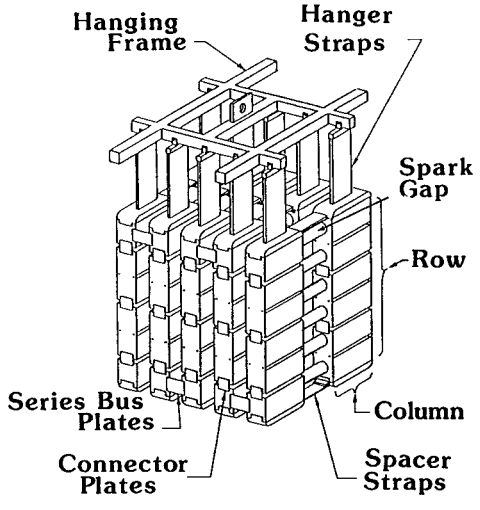

Figure 2 - PBFA II Marx Generator

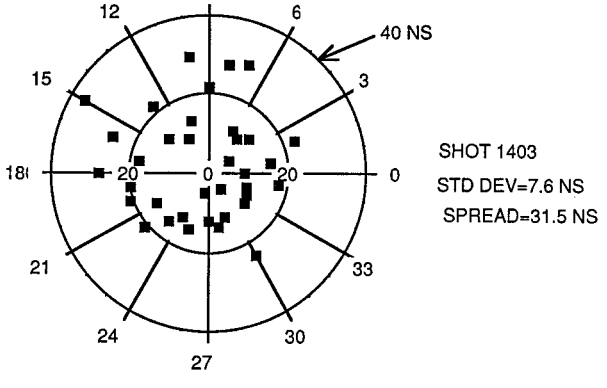

Figure 3 - PBFA II Marx Timing Plot

Due to the size and complexity of the Marx, it was the first system tested. A high-voltage testbed was constructed to provide initial qualification testing for all the Marxes after assembly. Each Marx was fired 20 times while the erection time and output voltage were measured. After this test, each Marx was hung in the main PBFA II annular tank awaiting the full Marx system test which occurred one year later. The full-system test was successfully completed several months before the December test shot and provided valuable data.

The performance of the PBFA II Marx generators is better than expected and easily meets our requirements. Typical spreads (the time between the first and last Marx firing) are less than 40 nanoseconds. A typical data set showing the Marx firing time as a function of location is shown as Fig. 3. With extra care and special procedures, timing spreads of less than 30 nanoseconds were also obtained.

Transfer Switches, Barriers and Control-Monitor Systems

The most serious failure for an accelerator of the PBFA-II type, is the rupture of an oil-water barrier and the subsequent mixing of the large quantities of transformer oil and deionized water. Previous experiments showed that an oil film coating on the aluminum parts in the water section lowers the electrical break-down strength by a factor of two. Conversely, water in the transformer oil can collect in the low spots of the Marx generators and cause arc overs and intermittent shorts during DC charging. In principle, the two liquids could be separated by a coalescer. In practice, the time for this separation would be measured in months. These factors make the oil-water interface a critical design feature of PBFA II.

The interface structure is shown in Fig. 4. The peak voltage without failure was 5.6 MV on the 1.4 meter diameter disk.

Ruptures of the oil-water interface can, in principle, be caused by many different failure modes. First, the barrier can track electrically and discharge the Marx across the insulator surface. This track dissipates energy which causes a rupture from the shock and the barrier breaks. This failure mode can be minimized by fabricating the barrier from a tough polymer such as polyurethane. The surface must be electrically graded properly and kept reasonably clean, especially at the triple points. Second, tracking and subsequent ruptures can be initiated from

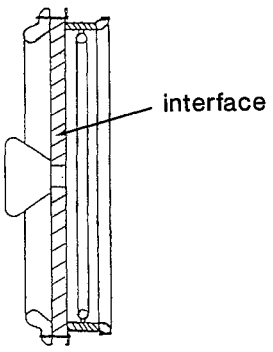

Figure 4 - The Oil-Water Barrier Interface

the Marx transfer switch. We prevent this failure mode by removing the barrier from the switch swing arm region and then providing a close-to-ground path for any swing arm discharge during transit. The swing arm transit time is also limited to less than 1.5 sec. The third failure mode is caused by a gas switch rupture which can couple a shock wave into the interface directly through the water capacitor inner cylinder. Multiple gas switch ruptures occur, for instance, if the triggering laser does not fire. During one test, 36 lines rang over to full voltage without a laser trigger. Nineteen gas switch housings tracked on the water side and exploded, thereby releasing their gas pressure energy into the water and the interfaces. Six other switches had heavy tracks, but did not break. Only one small oil-water interface leak was detected after this incident. To prevent this failure mode, the barrier must be designed to withstand gas switch explosions and, again, to be tough. During the checkout phase, the PBFA II interfaces have withstood all of these potential failure modes.

Another important operational feature is the firing inhibit ability of the Control and Monitor System (C/M) for PBFA II [5]. During the preparation of PBFA II for a shot, the C/M monitors the performance of key components on subsystems of the accelerator. If any of the monitored points fall out of tolerance, the C/M prevents the fire signal from activating the Marxes and other electrical subsystems. A shot can be successfully aborted up to a few microseconds before the expected firing. This C/M capability thus saves time and hardware. Several times during the countdown sequence the C/M stopped a trigger that would have put the accelerator at greater risk or that would have resulted in poor data. Typical monitoring points are: gas switch pressure, laser capacitor bank charge, Marx trigger generators, data acquisition trace condition, and the ion diode B-field bank voltage.

Water Capacitors

The original water capacitor was designed with a comfortable safety factor and then thoroughly checked on Demon through repeated test firings. Demon is a single-module prototype for PBFA II. Later in the program, extra gas switch length was needed and, subsequently, the original water capacitor was shortened by about 20%. This shortened length caused an unacceptable decrease in the energy transfer efficiency. After considering several alternatives, we decreased the outside diameter of the water capacitor to provide a capacity that was similar to that on the longer water capacitor. The decreased diameter outer cylinder increased the electrical fields significantly above those predicted safe by the J. C. Martin (JCM) water breakdown formula based on data by I. D. Smith [6]. Previous data on PBFA I and Proto II, along with a new theory of water breakdown [7], indicated that the new design (shown as Fig. 5) should not break down at our expected operating level. The JCM formula for water breakdown is

$$Ft^{1/3}A^{.1} = \begin{cases} .3 \text{ for positive surfaces and} \\ .6 \text{ for negative surfaces} \end{cases} \quad (1)$$

The formula values were determined from water breakdown data up to several times 10^4 square cm. and may not be applicable to very large systems.

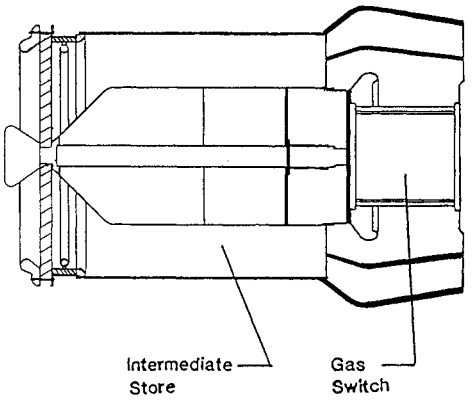

Figure 5 - Water Capacitor

The 36 PBFA II water capacitors have a total negative electrode area of 1.54×10^6 square cm. while the positive electrode total area is 2.71×10^6 square cm. The measured peak voltage on the water capacitors was 5.4 MV during the non-laser triggered ringover. Our JCM constants for this level are .393 for the positive electrode and .654 for the negative electrode, over the Formula (1) 30% and 9%, respectively, values which indicate that the area term scaling of .1 is too conservative for these large areas.

During the water capacitor testing and use, the only arc-overs that occurred were at the outer conductor and the grading structure at the high voltage end of the gas switch where the fields are slightly enhanced; a true large-area breakdown between cylinders has not yet been observed. In principle then, even these large numbers for the JCM constant may be too conservative.

In summary, a favorable situation exists for large area water breakdown. The JCM design formulae are pessimistic for large areas, and water-dielectric energy stores can be designed significantly smaller than were expected from the JCM formulae.

Laser Triggered Gas Switch

Based on experience with triggered gas switches on Hydra, Proto II [8], and PBFA I [9], we expected that considerable effort would be necessary to successfully make a 5 MV, highly synchronized (less than 15 ns spread), compact, low inductance, multi-channel, reliable gas switch. The research on the PBFA II LTS started before the first shot on PBFA I and is still in process. We were encouraged by the 10 ns total spread for the 36 modules that was finally achieved on PBFA I [9] using multistage electrically-triggered switches. However, due to the energy loss ($\sim$ 10%) due to the electrical trigger coil of the PBFA I 3 MV switches and the higher trigger voltages that would be needed for the 5 MV PBFA II gas switches, we decided to use a laser trigger.

Fortunately, laser triggered switches, originally pursued by A. H. Guenther and others at the Air Force Weapons Lab [10], provided timely developments that made laser triggering feasible for PBFA II. A group at Lawrence Livermore National Laboratory (LLNL) reported a 100 ps jitter from a .5 cm SF-6 insulated gap when triggered by a KrF laser [11]. A research program was started at Sandia to investigate the low jitter switching as applicable to PBFA II. Several UV and some IR laser triggered SF-6 insulated gaps were

tested and detailed in the literature [12,13,14]. In general, the requirement for low-energy, low-jitter LTS is that a large portion of the gas gap length should be ionized by the laser.

The PBFA II gas switches have more demanding requirements than other triggered switches. The switch inductance must be low (about 150 nh) and the peak currents must be .3 MA through each switch. This requirement comes from the use of the Double Bounce method of pulse compression, first suggested by Ian Smith of Pulsed Sciences Inc. (PSI), to relax the requirements on the self breakdown water switching needed to provide the fast output pulse [15]. Double bounce pulse compression will be discussed later. In addition, the gas switch housing length was limited to 68 cm by the position of the laser standpipe. A multiple channel gas switch would meet these requirements. We noted that a multistage switch forming several channels during breakdown was under test and performing well on SPEED [16]. This type of switch also fit well with the LTS requirements mentioned above since only a small fraction of the total gap length of the multistage switch needed to be triggered which, in turn, minimized the laser energy required [14].

The switch invented for PBFA II is called the Rimfire switch. It was named for the way the center switching elements are mounted and the way they break down. The Rimfire switch is shown in Fig. 6 [17].

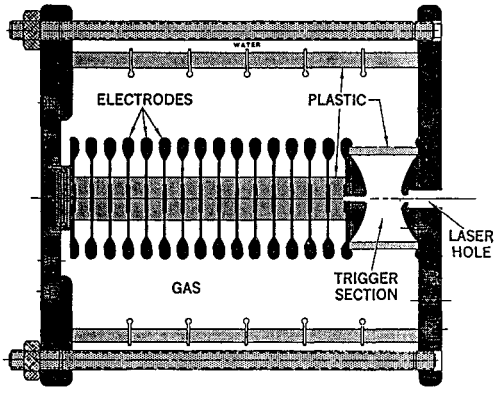

Figure 6 - Rimfire Switch

The Demon tests described previously [18] and the results described at this meeting [19] indicate that the present PBFA II switch should be operating satisfactorily. However, during the accelerator checkout the switch performance was not satisfactory. A typical shot timing record is shown as Fig. 7.

Figure 7 shows several features that allowed us to separate the problems contributing to the switching spread. The early switch breakdowns come from two sources. First, the multiple rimfire switch gaps can start to break down early. When the trigger pulse arrives, a large portion of the gap is already broken down and the switch runs faster when compared to the others. Second, and probably most frequent, prefires occur when the gas housing tracks electrically, either on the gas or water side, and closes the circuit outside of the gas switch electrodes.

Figure 7 also shows a nice center grouping of switches that run with a Gaussian-like distribution of breakdown times. This group of switches demonstrate the proper switch action. Although the spread is somewhat larger than expected, this grouping shows triggering.

Finally, Fig. 7 shows the late switches that were not strongly triggered. These switches might have had inappropriate laser energy and focusing or mechanical anomalies.

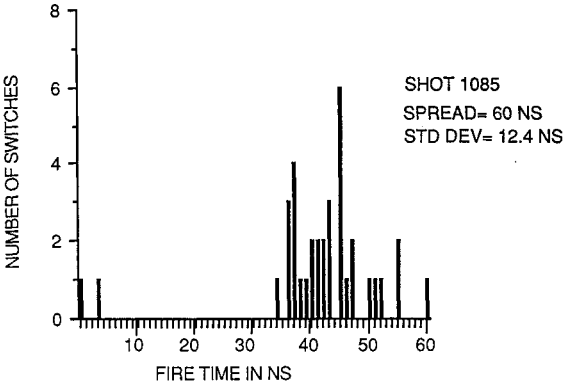

Figure 7 - PBFA II Typical LTS Performance

Two key parameters strongly affect the LTS operation. First is the switch electric field [19,20]. Second is the proportion of trigger gap distance that is ionized by the laser beam. A simple model was constructed, by T. H. Martin, from the J. C. Martin scaling relations [21]. If we assume that the laser spark of length, x, has the effect of reducing the gap length, d, to an effective gap d-x, then we find that:

$$\left(\frac{v}{d-x}\right) t_{eff}^{1/6} = \frac{k-}{(d-x)} \left(\frac{P}{P_o}\right)^n \qquad (2)$$

The running time of the switch changes as the field to the sixth power; or, for every 12% of field increase, the switch runs in one-half of the time. For instance, if 50% of the gap is ionized by the laser spark, then the effective trigger field is increased by a factor of two. The run time is, in turn, decreased by a factor of 64. We found that the laser spark length is a function of the focal length of the lens, the laser energy, and the laser wavelength [12].

We expect that an important factor for proper trigger gap operation is to assure that the laser pulse length is equal to or longer than the run time of the entire switch. During the construction of PBFA II, the input laser beam diameter was doubled from that of the Demon prototype to minimize damage and allow longer life and easier adjustment for the optical train. This seemingly minor change during the construction phase resulted in a shorter laser ionized path in the triggering gap which in turn resulted in the switches running slower. Some switches dropped out of the laser pulse time window and subsequently exhibited large spreads and jitters. The switches can be brought back to a faster runtime by either increasing the trigger gap field or lengthening the laser ionized path. A series of experiments outlining this effect is being presented by Turman and Wilson [19,20].

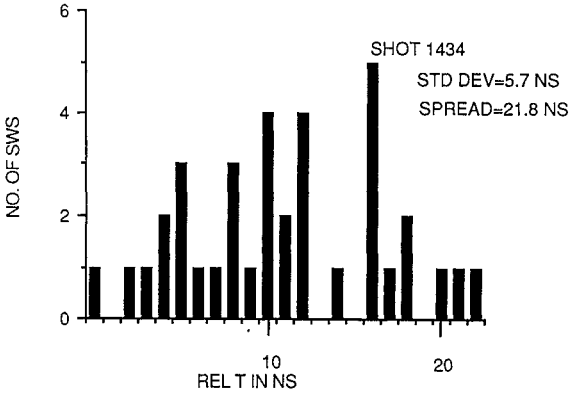

Figure 8 - PBFA II Latest Shot LTS Performance

The latest gas switch data, with only a change in the F-number of the laser beam, is shown as Fig. 8. The central group of switches has a one sigma distribution of 5.7 nanoseconds and a 22 nanosecond total spread at less than 70% of self-breakdown voltage, which is much closer to the values needed for PBFA II target experiments.

Water Switching, Pulse Forming, and Transmission Lines

The pulse forming and transmission lines are configured on PBFA II to enable pulse compression and voltage addition. The pulse forming lines are switched by self breakdown water switches. Multiple-module voltage addition allows high voltages to be provided in a water dielectric. Since the velocity of electrical waves in water is one-ninth that in vacuum, the pulse forming lines and switching hardware, in physical size, can constitute an appreciable portion of a pulse length. A high voltage pulse of energy (if one could see it) in water looks more like a 2 meter-thick slab of energy converging into the center of the accelerator. Switching and adding smaller, individual slabs of energy from the 36 modules is a challenging task that always loses energy. A PBFA II module line is shown in Fig. 9.

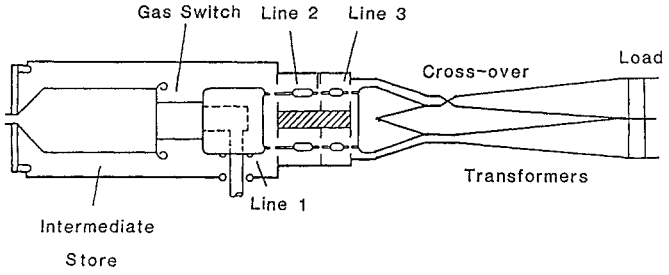

Figure 9 - PBFA II Line

The water switching on PBFA II has performed well. Early in the program, switch energy losses were not well known and large inefficiencies were a concern. After reviewing previous data from Sandia and elsewhere, we concluded that if the average field on the water switch could be high (by using de-enhanced switch points) then the energy losses would be acceptable. Our present line 1 switch has 4 individual switches that are gapped to 10 cm. The average field is 0.45 MV/cm at a peak voltage of 4.5 MV. The double bounce charging system on line 1 was intended to provide a fast rise voltage to a voltage plateau of about half of the desired voltage when the main forward-going pulse arrives at the switch pins. The main pulse reflects from the open-water switches back to the gas switch inductance. The pulse again reflects from the gas switch inductance back towards the water switches. The water switches then close just prior to the arrival of the multiple-reflected pulse [14].

One item that limits our ability to construct a double bounce water switching system is the stray capacity across the gas switch. Double bounce relies on making large impedance discontinuities at both ends of line 1. Stray capacities between the ends of the line cylinders make obtaining these discontinuities more difficult than expected. Specifically, the stray capacity across the gas switch is important, and the stray capacity between line 1 and its ground plate was significant. Both of these capacities were minimized.

If standard energy transfer were used (1-cos ωt) then the peak voltage on line 1 would approach 6 MV in 200 nsec. This would require a water switch gap of 20 cm which would be impossible to package within this configuration. The double bounce charging allowed a 10 cm gap to perform the same switching at 4.5 MV and 120 nsec charge time. In summary, double bounce has allowed the use of water switching in this accelerator. Figure 10 presents data showing that double bounce water switching is working.

The water switching exhibits low jitter. Figure 10 shows a plot of a single line average switch breakdown time as a function of the gas switch breakdown time. If a gas switch closes late, then its water switches will close in a relatively shorter time due to a higher applied voltage and, therefore, reduce the overall module jitter. This behavior was observed in our tests. The deviation about a straight line approximation of this relationship is an approximation to the water switch jitter. This particular data set shows a water switch jitter of 3.5 ns and is typical.

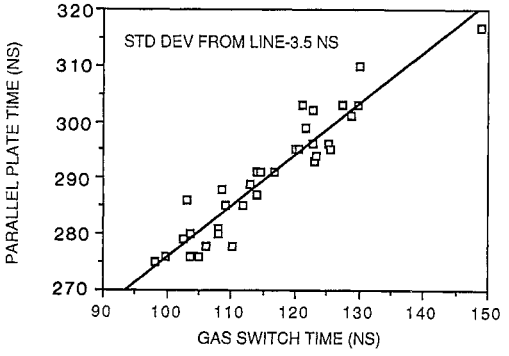

Figure 10 - Water Switch Jitter

A brief description of the voltage adding method will be given next. After the electrical pulses are formed in lines 1 and 2 [15], the energy is evenly divided into two flat-plate transmission lines. One of the flat plate transmission lines has a crossover which inverts the voltage vector on that side. The two voltage vectors are now in the same direction and they can be added in series to produce the voltage sum. The addition takes place by bringing each flat-plate line into an impedance step-up line transformer and then adding the transformer lines in series at the insulator stack wall. At the stack wall, each module's lines are joined with other module's outputs which are connected in similar fashion. Practical considerations, such as stray capacities, limit our ability to stack these lines to arbitrarily high voltages.

An energy-loss mechanism that occurs while adding line voltage was discovered. With two flat-plate lines with opposing voltages, the energy is carried mainly between the two plates of each line as given by the Poynting vector. The magnetic field lines close on themselves between the lines shown as Fig. 11a. This figure represents the flux lines as viewed from the end of two transmission lines carrying energy in the same direction. Energy is transported with relatively small loss in this configuration.

In a configuration where the voltages are to be added, one voltage must be inverted between one set of line plates. The magnetic field lines now close on themselves between the two sets of lines and we find that considerable energy is carried external to the parallel plates as shown in Fig. 11b. In PBFA II (or any voltage adding device with open transmission lines) this energy between lines runs into a short circuit when the lines are connected (at the insulator stack in our design). Unfortunately, most of this external energy is then lost by being reflected away from the connection [22].

An additional loss was caused when impedance transforming lines were used to further step up the voltage to drive the inductive load. As the lines separate to increase the impedance and voltage, proportionally more energy is carried on the backside

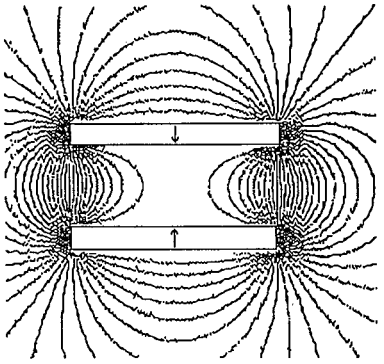

A-VOLTAGE VECTORS OPPOSING
LOW ENERGY BETWEEN LINES

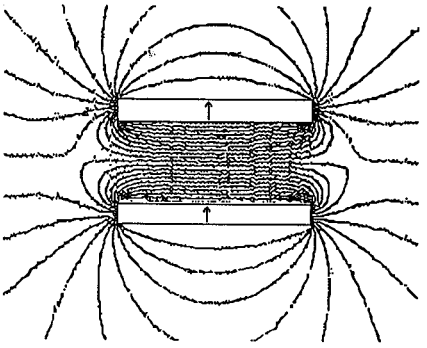

B-VOLTAGES ADDING
MORE ENERGY BETWEEN LINES

Figure 11a, b - Line Field Configurations

of the lines. Subsequently, even more energy is lost at the stack connection when impedance transforming lines are used.

The final energy loss comes from the inherent inefficiency due to driving an inductive energy store from a transmission line. Energy that is not coupled into the inductor is reflected away from the load.

Presently we are conducting an energy flow study to determine if simple modifications can be made to the lines of PBFA II to increase the energy efficiency.

The output energy from each of these modules into an inductive load is between 80 and 90 kilojoules. An open circuit voltage waveform that was calculated from data on one shot is shown as Fig. 12. One half of this voltage could be delivered to a 2.2 ohm load.

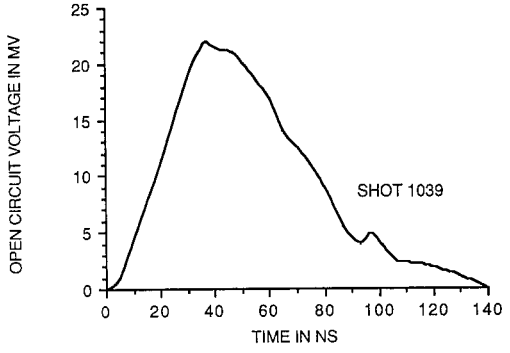

Figure 12 - PBFA II Open Circuit Voltage

Inductive Energy Store and the POS

Figure 13 shows the region of the accelerator that houses the inductive store. The current path (and the inductor) consists of four parts: first, the equivalent lumped inductance of the water portion of the transmission line transformer; second, the insulator stack; third, the vacuum-transmission line voltage adder; and last, the POS inductance.

Of these four parts of inductance, only the energy in the vacuum-transmission line voltage adder can be provided to the diode load. When the POS opens, the high voltage pulse propagates back down the voltage adder until it arrives at the insulator stack. At the arrival time, the insulator flashes and crowbars the vacuum side of the insulator stack. This crowbar does not allow the energy stored in the plastic portion of the insulator stack or the water section to flow to the load. The approximate circuit for the inductive energy storage section is shown as Fig. 14.

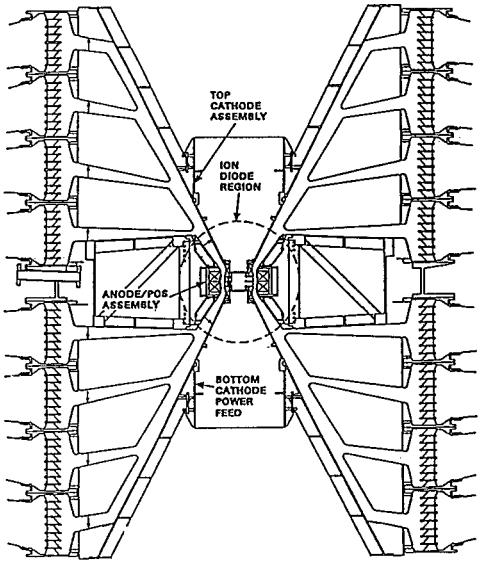

Figure 13 - Insulator Stack, Vacuum Voltage Adder, and POS

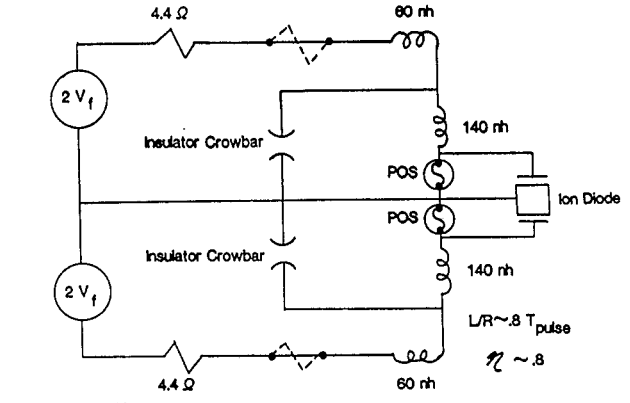

Figure 14 - Inductive Store Circuit Diagram

The peak current provided to drive this inductive load is a measure of the amount of energy that the transmission lines are providing. If the POS remains shorted through the time of peak current, then the data are valid for determining the forward-going energy. Figure 15 shows the actual measured total current and the simulated peak currents for the properly phased 80 kJ per module input for one half of the accelerator. As can be seen, the data and simulation agree.

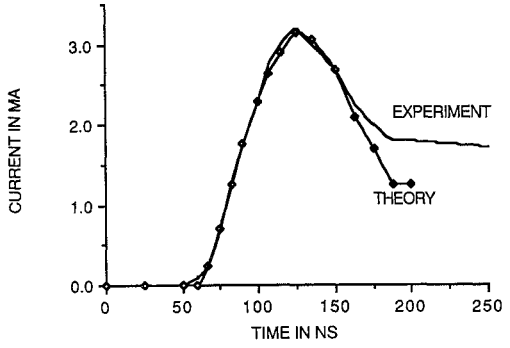

Figure 15 - POS Peak Current

The peak current achieved is indicative of the vacuum adder efficiency. For the currents shown as Fig. 15 theory, a voltage adder efficiency of 100% (within experimental error) was found. This is in keeping with the predictions [23].

A more detailed drawing of the POS and diode area is shown as Fig. 16 [24]. There is one POS for each half of the accelerator. The POS is a type of vacuum opening switch which uses plasma injected into a section of the vacuum power feed to conduct current up to a predetermined level before opening. Under the optimum conditions, a POS can open to an impedance that is many times the generator impedance within 5 to 15 nsec after conducting currents of several megamps for several tens of nanoseconds.

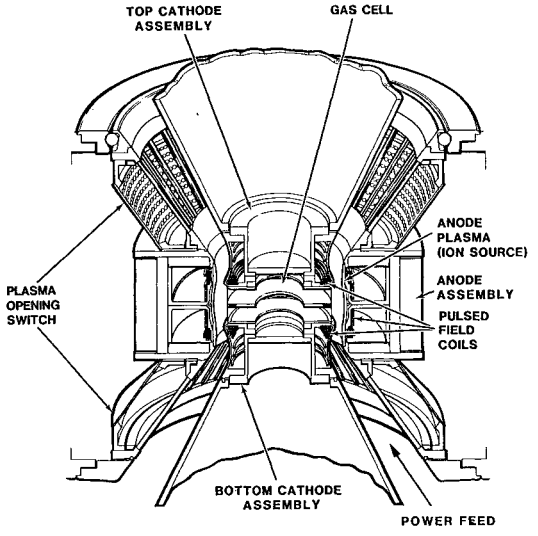

Figure 16 - POS-Diode Drawing

The POS system on this accelerator uses a newly developed flashboard plasma source to provide the plasma necessary to conduct more than 3 MA in each switch. The POS system on PBFA II is unique because of its size and the operating voltage. This POS system is intended to operate at current, voltage, and power levels of up to 7 MA, 30 MV, and 125 TW.

Many processes are required for a POS to perform as an opening switch [25,26]. The processes include current penetration into the switch plasma, electrode sheath formation, magnetic-pressure driven convection, plasma-erosion, and magnetic insulation. The conduction phase is controlled by the switch plasma conditions, the switch current, and the geometry. When the switch opens, erosion and probably hydrodynamic effects cause a small gap to open between the cathode and the switch plasma. When a large enough gap opens, then current begins to flow to the load, and this current tends to direct the cathode electrons back to the cathode. As the switch continues to open, even more of the current is diverted to the load and the switch opens even faster. The POS's ability to operate is a function of its load. The POS has become a useful pulsed power tool used in several applications such as prepulse suppression [25,27], pulse shaping [28,29], and voltage and power gain [30,31].

Opening switch performance achieved to date is shown in Fig. 17 [32]. Multiple B-dots are located on both the anode and cathode. These B-dots are located upstream and downstream of the POS. By this instrumentation method, the upstream (input current) and downstream (switched current) can be measured. The data for this figure was taken with a 16 nh load. Figure 17 shows a good efficiency for switching currents. However, a more thorough review of the data shows that there is a rather large plasma non-uniformity around the cathode azimuth. We are presently developing more uniform plasma sources and methods to accurately monitor the gap plasma [24].

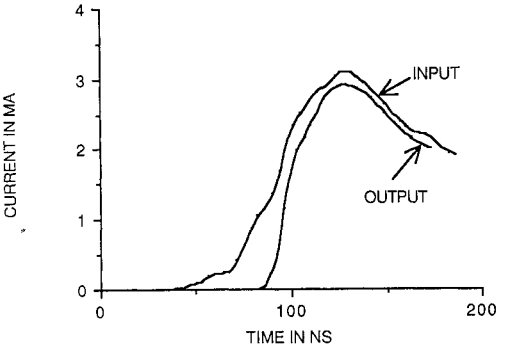

Figure 17 - POS Performance

The POS current efficiency into the 16 nh load, as shown in Fig. 17, is better than 90%. The results for higher impedance loads have not exceeded 60%. The reason for the lower efficiency is being studied. Likely causes for the lower efficiency are the non-uniform plasma density in the switch and the difficulty in transmitting the power through MITLs to high-impedance loads such as ion diodes.

We are working to improve the plasma density variation from the flashboards to less than a factor of two in azimuth. In addition, plasma-filled loads are being tested to provide a low impedance at the beginning of the POS output current. We believe that the POS is providing data that indicates proper operation. Ultimately, the POS should perform well into an ion diode with the proper impedance to provide both voltage and power gain.

Summary

The PBFA II pulsed power is performing almost as expected. The Marx generators are operating very well, and this particular design could be extended into even higher energy levels if needed. The laser triggered gas switching, after not performing to expectations, appears to be operating and is extendable to even larger systems. Anticipated mechanical shock problems with the laser optics did not occur. The water switching is working with low energy loss and jitter. The output energy of PBFA II has been measured, and losses are occurring during the voltage addition in the water section. The reasons for the losses are understood, and a portion of the presently lost energy is recoverable. The first high power (~ 100 TW), fast-rise current (4×10^{14} A/sec), 2 MJ POS shows indications of operating. However, further testing must be done in this area.

Presently, as intended, PBFA II is being used to conduct ion diode studies.

Acknowledgements

This program was sponsored by the Department of Energy and managed by the office of Inertial Fusion. With their help and assistance, this large state-of-the-art accelerator was brought into existence. We thank the Naval Research Laboratory for their many contributions to our POS program and look forward to their continuing assistance.

This work was supported by the U. S. Department of Energy under Contract Number DE-AC04-76DP00789.

References

[1] J. M. Wilson, "PBFA II Energy Storage Section Design," Proc. of the 1983 IEEE Pulsed Power Conf.

[2] J. M. Wilson and R. R. Johnston, "PBFA II Energy Storage System Configuration and Characteristics," Proc. of the 1985 IEEE Pulsed Power Conf.

[3] J. M. Wilson, "PBFA II Energy Storage System Performance and Operation," Proc. of the 6th IEEE Pulsed Power Conf.

[4] T. H. Martin, "The Hydra Electron Beam Generator," IEEE Trans. on Nuclear Science, vol. NS-20, No. 3, June 1973.

[5] V. M. Italiano, "Providing Automated Control for PBFA II," Proc. of the 1985 IEEE Pulsed Power Conf.

[6] J. C. Martin, "Nanosecond Pulse Techniques," Circuit and System Design Notes 4, April 1970, Atomic Weapons Research Establishment, Aldermaston, England.

[7] T. H. Martin, Unpublished Notes on Water Breakdown.

[8] T. H. Martin, J. P. VanDevender, D. L. Johnson, D. H. McDaniel, and M. F. Aker, "Proto II - A Short Pulse Water Insulated Accelerator," First Int. Conf. on Electron Beam Research and Technology, Albuquerque, NM, November 1975, Sandia National Labs publication SAND76-5122.

[9] D. D. Bloomquist, G. R. Montry, S. E. Downie, and G. R. Peterson, "Cascade Switch Implementation on PBFA I," Proc. of the 1985 IEEE Pulsed Power Conf.

[10] A. H. Guenther and J. R. Bettis, "The Laser Triggering of High-Voltage Switches," J. Phys., vol. D 11, p. 1577 (1978).

[11] W. R. Rapoport, J. Goldhar, and J. R. Murry, "KrF Laser-Triggered SF-6 Spark Gap for Low Jitter Timing," IEEE Trans. on Plasma Science, vol. PS-8, 167 (1980).

[12] J. R. Woodworth, R. G. Adams, and C. A. Frost, "UV-Laser Triggering of 2.8 Megavolt Gas Switches," IEEE Trans. on Plasma Science, vol. PS-10, No. 4, December 1982.

[13] J. R. Woodworth, P. J. Hargis, Jr., L. C. Pitchford, and R. A. Hamil, "Laser Triggering of a 500-kV Gas-Filled Switch: A Parametric Study," J. Appl. Phys. 56, p. 1382, Sept. 1984.

[14] R. G. Adams, W. B. Moore, J. R. Woodworth, M. M. Dillon, F. Morgan, K. J. Penn, "Ultraviolet Laser Triggering of A 5 Megavolt Multistage Gas Switch," Proc. of the 1983 IEEE Pulsed Power Conf.

[15] B. N. Turman, T. H. Martin, E. L. Neau, D. R. Humphreys, D. D. Bloomquist, D. L. Cook, S. A. Goldstein, L. X. Schneider, D. H. McDaniel, J. M. Wilson, R. A. Hamil, G. W. Barr, and J. P. VanDevender, "PBFA II, A 100 TW Pulsed Power Driver for the Inertial Confinement Fusion Program," Proc. of the 1985 IEEE Pulsed Power Conf.

[16] J. F. Seamen, J. P. VanDevender, D. L. Johnson, T. H. Martin, G. Zawadzkas, E. L. Neau, W. Beezhold, K. Mikkelson, S. Downie, D. Green, "SPEED, A 2.5 TW, Low Impedance Pulsed Power Research Facility," Proc. of the 1983 IEEE Pulsed Power Conf.

[17] D. R. Humphreys, K. J. Penn, J. S. Cap, R. G. Adams, J. F. Seamen, and B. N. Turman, "Rimfire: A Six Megavolt Laser Triggered Gas-Filled Switch for PBFA II," Proc. of the 1985 Pulsed Power Conf.

[18] B. N. Turman, W. B. S. Moore, J. F. Seamen, F. Morgan, J. Penn, and D. R. Humphreys, "Development Tests of a 6 MV, Multistage Gas Switch for PBFA II," Proc. of the 1983 IEEE Pulsed Power Conf.

[19] B. N. Turman and D. R. Humphreys, "Scaling Relations for the Rimfire Multi-Stage Gas Switch," Proc. of the 6th Pulsed Power Conf.

[20] J. M. Wilson, G. L. Donovan, "Laser-Triggered Gas Switch Improvements on PBFA II," Proc. of the 6th Pulsed Power Conf.

[21] T. H. Martin, "Pulse Charged Gas Breakdown," Proc. of the 1985 IEEE Pulsed Power Conf.

[22] W. A. Johnson, E. L. Neau, and L. X. Schneider, "TEM Analysis and Computer Simulations of Demon and PBFA II Open Transmission Line Systems," Proc. of the 6th IEEE Pulsed Power Conf.

[23] D. H. McDaniel, R. W. Stinnett, and E. W. Gray, B. E. Mattis, "Design and Optimization of the PBFA II Vacuum Interface and Transmission Lines for Light Ion Fusion," Proc. of the 1985 IEEE Pulsed Power Conf.

[24] R. W. Stinnett, D. H. McDaniel, G. E. Rochau, W. B. Moore, E. W. Gray, T. J. Renk, H. N. Woodall, T. W. Hussey, S. S. Payne, R. J. Commisso, J. M. Grossmann, D. D. Hinshelwood, R. A. Meger, J. M. Neri, W. F. Oliphant, P. F. Ottinger, B. V. Weber, "Plasma Opening Switch Development for the Particle Beam Fusion Accelerator II (PBFA II)," Proc. of XII Int. Symp. on Discharges and Electrical Insulation in Vacuum, 1986.

[25] C. W. Mendel Jr., and S. A. Goldstein, "A Fast-Opening Switch for Use in REB Diode Experiments," J. Appl. Phys., 48, 1004 (1977).

[26] P. F. Ottinger, S. A. Goldstein, and R. A. Meger, "Theoretical Modeling of the Plasma Erosion Opening Switch for Inductive Storage Applications," J. Appl. Phys., 56, 774 (1984).

[27] P. A. Miller, J. W. Poukey, and T. P. Wright, "Electron Beam Generation in Plasma-Filled Diodes," Phys. Rev. Lett., 35, 940 (1975).

[28] R. Stringfield, R. Schneider, R. D. Genuario, I. Roth, K. Childers, C. Stallings, and D. Dakin, "Plasma Erosion Switches With Imploding Plasma Loads on a Multi-terawatt Pulsed Power Generator," J. Appl. Phys., 52, 1278 (1981).

[29] R. W. Stinnett, W. B. Moore, R. A. Meger, J. M. Neri, and P. F. Ottinger, "Plasma Opening Switch Experiment on PBFA-I," Bull. Am. Phys. Soc., 29, 1207 (1984).

[30] R. A. Meger, R. J. Commisso, G. Cooperstein, and S. Goldstein, "Vacuum Inductive Store/Pulse Compression Experiments on a High Power Accelerator Using Plasma Opening Switches," Appl. Phys. Lett., 42, 943 (1983).

[31] B. V. Weber, J. R. Boller, R. J. Commisso, J. M. Grossmann, D. D. Hinshelwood, R. A. Meger, J. M. Neri, W. F. Oliphant, P. F. Ottenger, T. J. Renk, S. J. Stephanankis, and F. C. Young, "Progress in Plasma Erosion Opening Switch Research at the Naval Research Laboratory," Proc. of 1985 IEEE Pulsed Power Conf.

[32] G. E. Rochau, D. H. McDaniel, W. B. S. Moore, G. R. Mower, T. R. Renk, H. N. Woodall, "Status of Plasma Opening Switch Development on PBFA II," Proc. of the 6th IEEE Pulsed Power Conf.